Journal of Alloys and Compounds 504S (2010) S102–S105

Contents lists available at ScienceDirect

Journal of Alloys and Compounds

journal homepage: www.elsevier.com/locate/jallcom

Plasticity enhancement of $Mg_{58}Cu_{28.5}Gd_{11}Ag_{2.5}$ based bulk metallic glass composites dispersion strengthened by Ti particles

J.S.C. Jang[a,*], Y.S. Chang[a], T.H. Li[a], P.J. Hsieh[a], J.C. Huang[b], Chi Y.A. Tsao[c]

[a] Department of Mechanical Engineering, Institute of Materials Science and Engineering, National Central University, Chung-Li 320, Taiwan, ROC
[b] Department of Materials and Optoelectronic Science, Center for Nanoscience and Nanotechnology, National Sun Yat-Sen University, Kaohsiung 804, Taiwan, ROC
[c] Department of Materials Science and Engineering, National Cheng Kung University, Tainan, Taiwan, ROC

ARTICLE INFO

Article history:
Received 23 June 2009
Received in revised form 2 March 2010
Accepted 3 March 2010
Available online 9 March 2010

Keywords:
Bulk metallic glass
Glass forming ability
Composite
Mechanical performance
Plasticity

ABSTRACT

We have successfully synthesized the Ti particles reinforced $Mg_{58}Cu_{28.5}Gd_{11}Ag_{2.5}$ metallic glass composites (BMGCs) rods with a diameter of 2–4 mm by injection casting method in an Ar atmosphere. The glass forming ability (GFA) and the mechanical properties of these Mg-based BMGCs have been systematically investigated as a function of volume fraction (V_f) of Ti particles. The results show that the compressive plasticity increases with the volume fraction of Ti particles. A drastic improvement of compressive plastic strain (reach up to 24%) occurs at the Mg-based BMGC with 40 vol.% Ti particles. In parallel, multiple shear bands were revealed on the sample surface after compression test. This suggests that these dispersed Ti particles can highly absorb the energy of shear banding and branch the primary shear band into multiple shear bands, thus decrease the stress concentration for further propagation of shear band and so as to significantly enhance plasticity. Additionally, the yield strength can be kept at 800 MPa as increasing the addition of Ti particles to 40 vol.%. This was found presumably due to the good bonding of interface between the Ti particle and amorphous matrix.

© 2010 Elsevier B.V. All rights reserved.

1. Introduction

Mg-based bulk metallic glasses (BMGs) have attracted great attention recently because of its low density and high damping capacity as compared to most other bulk metallic glasses (BMGs), such as the Pd, Zr, and Fe-based amorphous alloys [1–3]. However, the Mg-based BMGs do not exhibit appreciable plastic deformation in a uniaxial mode, they tend to break into pieces before yielding [4–7]. Therefore, the improvement on plasticity has been strongly requested for the progress in the application of Mg-based BMGs. To solve the brittleness of Mg-based BMGs, the development of bulk metallic glass composites (BMGCs) with micro- or nano-scaled second phase dispersed homogeneously in a BMG matrix have been proven to be an effective way for improving plasticity. Two main approaches of forming BMGCs have been explored so far, one is to in situ precipitate crystalline phases in the BMG matrix, the other is to ex situ introduce foreign particles (i.e., metallic or refractory ceramic particles) into the BMG matrix [2,8–14]. In Mg-based alloys, the first development of Mg-based BMGC, a $Mg_{65}Cu_{7.5}Ni_{7.5}Zn_5Ag_5Y_{10}$ with Fe dispersoid, was reported by Ma et al. in 2003 [2]. Since then, many other types of Mg-based BMGCs have been developed with ceramic and metallic particles (e.g., TiB_2 [15], ZrO_2 [16], WC [17], SiC [18], and Nb [19], porous Mo [20], Ti [21], and Fe [22]) and all exhibits remarkable plasticity improvement. Among these developed Mg-based BMGCs, the $Mg_{65}Cu_{25}Gd_{10}$/40 vol.% Ti BMGC displays the highest plastic strain of 41% [21]. However, this BMGC presents much low value of yield strength (470 MPa) than the base BMG (850 MPa). This differs from the phenomena of the $Mg_{58}Cu_{28.5}Gd_{11}Ag_{2.5}$/25 vol.% porous Mo BMGC, possessing much higher yield strength than the base BMG [20]. Therefore, we believe that there exist some factors which may significantly affect the mechanical performance of these Mg-based BMGC, including particle size, vol. fraction, and interface between the particle and the glassy matrix. Accordingly, the composition of $Mg_{58}Cu_{28.5}Gd_{11}Ag_{2.5}$ which posses high GFA [20] is selected as the raw alloy for preparing the BMGC by reinforcing with ductile Ti particles (which has spherical shape) in this study. The effect of particle size, vol. fraction, and the interface between the particle and the glassy matrix on the mechanical performance of these BMGCs were investigated.

2. Experimental details

The composition of $Mg_{58}Cu_{28.5}Gd_{11}Ag_{2.5}$ was selected as the raw alloy for preparing the BMG composites. High purity Cu and Gd (>99.9 wt.%) were pre-alloyed into Cu–Gd alloy ingot by arc melting in a Ti-getted argon atmosphere. Then the Cu–Gd alloy was melted together with high purity Mg and Ag pieces to obtain the tar-

* Corresponding author at: Department of Mechanical Engineering, Institute of Material Science and Engineering, National Central University, #300, Chung-Li City 320, Taiwan, ROC.
E-mail address: jscjang@ncu.edu.tw (J.S.C. Jang).

0925-8388/$ – see front matter © 2010 Elsevier B.V. All rights reserved.
doi:10.1016/j.jallcom.2010.03.030

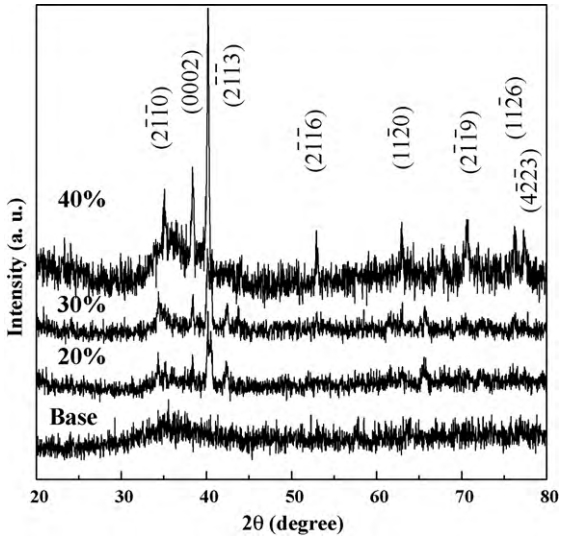

Fig. 1. XRD pattern of the $Mg_{58}Cu_{28.5}Gd_{11}Ag_{2.5}$ BMGC with different vol.% of Ti particles.

get composition by induction melting under argon atmosphere. While melting, high purity Ti particles with spherical shape were added into the matrix alloy under argon atmosphere. Mechanical stirring was exerted to enhance the homogeneous mixing of the particles with the melt. The particle size and vol. fraction of Ti particle range from 44 μm to 75 μm and 20 vol.% to 40 vol.%, respectively. Furthermore, the composite alloy ingot was remelted by induction melting in a quartz tube and injected into a water-cooled Cu mold by argon pressure to obtain BMGC rods with sizes of 2–4 mm in diameter. The thermal properties of the monolithic BMG and BMGCs were characterized by TA Instruments DSC 2920 differential scanning calorimeter (DSC) under flowing purified argon with a heating rate of 20 K/min. The structure of the specimen was characterized by Scintag X-400 X-ray diffractometer with monochromatic Cu Kα radiation and transmission electron microscopy (TEM, Philip, Tecnai G2 at 200 keV). TEM specimen was prepared by dimpling and ion milling method. The compression tests were performed at a strain rate of $5 \times 10^{-4}\,s^{-1}$ by a MTS 810 mechanical test system. The compression samples with the height to diameter ratio of 2:1 ($h = 8$ mm/$d = 4$ mm, and $h = 4$ mm/$d = 2$ mm) were cut to be parallel and carefully polished to insure the flatness from the as-cast BMG and BMGC rods. The distribution of Ti particles in the amorphous matrix of BMGC and the morphology of fracture surface were examined by a Hitachi S-4700 field emission scanning electron microscope (FEG-SEM) with energy-dispersive spectroscopy (EDS) capability.

3. Results and discussions

Since the melting temperature of Ti element (1941 K) is much higher than the liquidus temperature of the $Mg_{58}Cu_{28.5}Gd_{11}Ag_{2.5}$

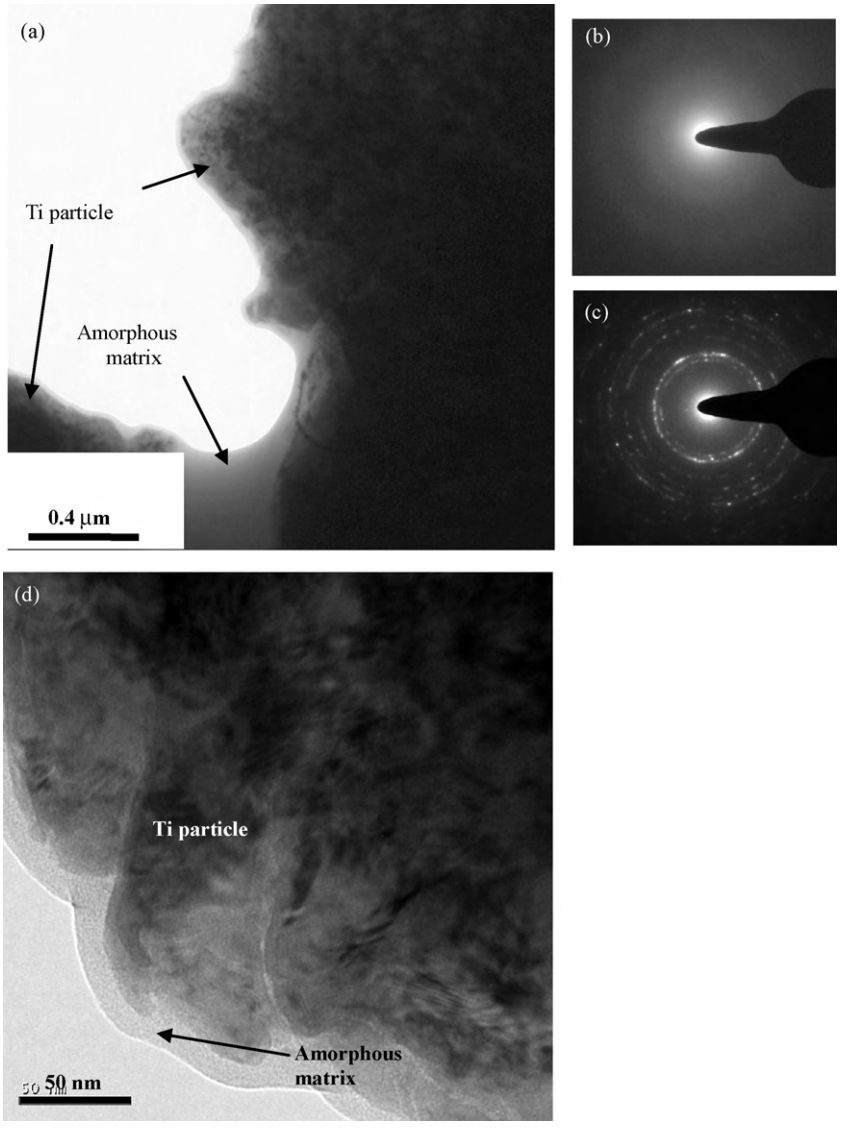

Fig. 2. (a) Bright field TEM image of Ti particles mounted with amorphous matrix, (b) SAD of amorphous matrix, (c) SAD of Ti particle, and (d) bright field TEM image of interface between Ti particle and amorphous matrix for the sample of $Mg_{58}Cu_{28.5}Gd_{11}Ag_{2.5}$ BMGC/40 vol.% Ti particles.

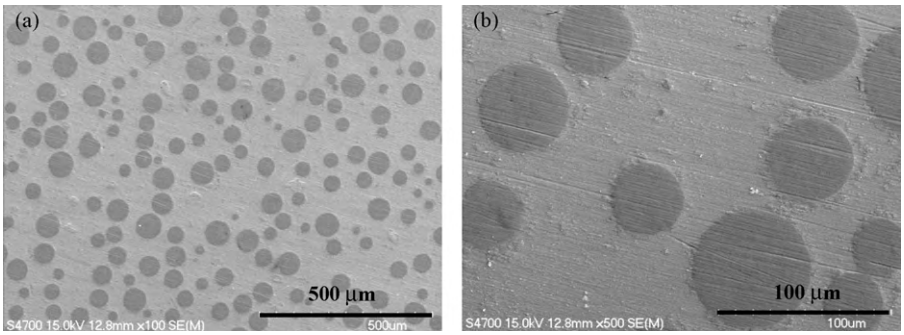

Fig. 3. SEM images of the cross-section for the $Mg_{58}Cu_{28.5}Gd_{11}Ag_{2.5}$ BMGC rods with 40 vol.% of Ti particles; (a) low magnification and (b) high magnification.

alloy (714 K), that Ti powders display almost immiscible with this Mg-based alloy during melting and casting process. Therefore, the results of DSC analyses revealed that all of these Mg-based BMGCs with different vol.% Ti particles would keep almost the same thermal properties as the based $Mg_{58}Cu_{28.5}Gd_{11}Ag_{2.5}$ BMG, presenting the nearly the same GFA around $\gamma = 0.42$ and $\gamma_m = 0.75$. This implies that the addition of Ti particles did not affect the matrix composition and no obvious chemical reaction has occurred to deteriorate the GFA. In addition, the XRD patterns of the Mg-based BMGCs with different vol.% Ti particles also demonstrate that the amorphous matrix phase with the broadened and diffused humps. No apparent crystalline peak is detected except the high intensity crystalline peaks from the Ti particles, as shown in Fig. 1. Moreover, a typical amorphous image with the halo ring of selected area diffraction pattern which mounted with Ti particles was observed from the Mg-based BMGC/40 vol.% Ti particles specimen by TEM, as illustrated in Fig. 2(a)–(c). The evidence of good bonding condition of Ti particle with the amorphous matrix can be seen from the clean interface between Ti particle and amorphous matrix as illustrated in Fig. 2(d).

The SEM observations of the polished cross-sectional surface of one typical Mg-based BMGC rod containing with 40 vol.% Ti particles are shown in Fig. 3. These Ti particles, with spherical shape and in the size range of 40–75 μm, not only homogeneously disperse in the metallic glassy matrix (Fig. 3(a)), but also present a very good bonding condition with the amorphous matrix as shown in Fig. 3(b). The final volume fraction of the Ti particles in the composite estimated by the image analysis was found very close to the added vol.% of Ti particle.

The hardness as a function of vol.% of Ti particles for the Mg-based BMGCs is shown in Fig. 4. The hardness displays a slight decreasing trend with vol.% of Ti particles due to the inherent low hardness of pure Ti (Hv 168) in comparison with the amorphous matrix (Hv 270). However, the hardness of these Mg-based composites is in agreement with the rule of mixture of the particular-reinforced composite materials. On the other hand, the compression tests revealed that a drastic improvement in plastic strain of the Ti particles reinforced Mg-based BMGCs. When the volume fraction of Ti particles increases to 30 vol.%, the Mg-based BMGC begins to exhibit clearly large enhancement of plasticity with true compressive plastic strain up to 12%, and a more remarkable increase in plastic strain up to 24% was obtained at the Mg-based BMGC with 40 vol.% Ti particles, as shown in Fig. 5. At the same time, these BMGCs present small decrease in yield strength and keeps at the value of 800 MPa. Multiple compression tests were conducted for confirming the reproducible trend and the scattering of the stress and strain was less than ±5% or less than ±40 MPa and ±5% or around ±0.5% engineering strain, respectively. In addition, it is worth to note that the BMGC with above 20 vol.% Ti particles presents distinct work hardening behavior after the yielding due to the work hardening nature of Ti phase. The ultimate compressive strength up to 945 MPa can be obtained at 40 vol.% sample. Though the performance of Ti contained Mg-based BMGC is not as strong as the porous Mo contained Mg-based BMGC [20], with 10% plastic strain and 0.95 GPa yield strength, but it performs much better plasticity than the 8 vol.% solid Nb particle-reinforced Mg-based BMGC (12% plastic strain) [19] and exhibits much higher yield strength than the 40 vol.% Ti particle-reinforced $Mg_{65}Cu_{25}Gd_{10}$ BMGC (about 470 MPa yield strength) [21]. Accordingly, the low density Ti particle (compare to Nb and Mo particle) still has the strong potential to apply on strengthening the Mg-based BMGs for the consideration of materials density.

In order to clarify the mechanism of significant plasticity enhancement in Mg-based BMGC, the SEM observations on the fracture surface were conducted to evaluate the function of the

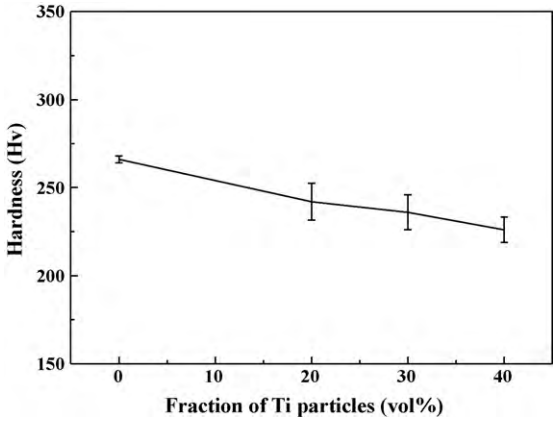

Fig. 4. Hardness as a function of vol.% of Ti particles for the $Mg_{58}Cu_{28.5}Gd_{11}Ag_{2.5}$ BMGCs.

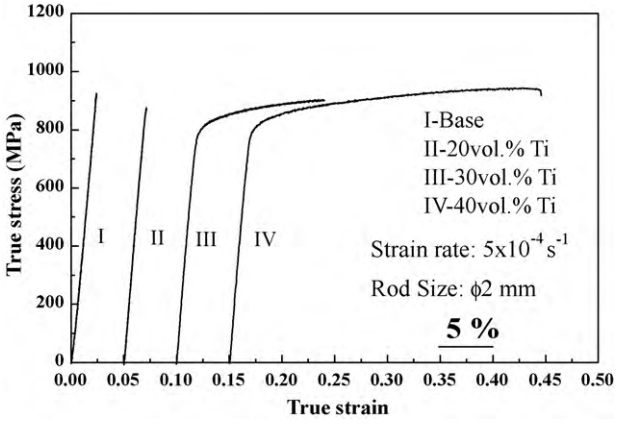

Fig. 5. True compressive stress–strain curves for the Mg-based BMG and BMGC with different vol.% of Ti particles.

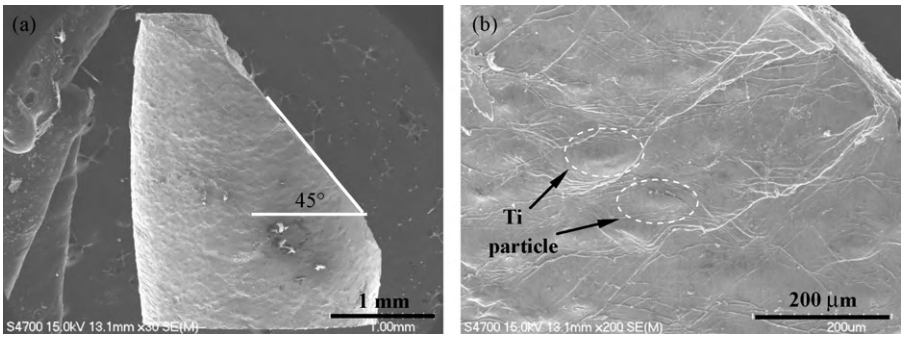

Fig. 6. SEM micrographs of (a) the fractured specimen and (b) specimen surface near the fracture area after compression test for the Mg-based BMGC/40 vol.% of Ti particles with 24% plastic strain.

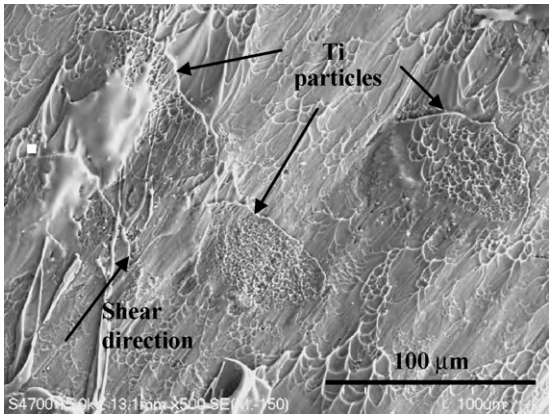

Fig. 7. SEM micrographs of the fracture surface of the Mg-based BMGC/40 vol.% of Ti particles.

"ductile Ti particles" on the improvement of mechanical performance. The observations on the specimen surface near the fracture area (Fig. 6) indicate the deformation follows a shear band mechanism. Fig. 6(a) shows the fractured specimen with a fracture surface oriented about 45° to the loading axis. The multiple shear bands can be observed along the fracture surface and around the Ti particles as shown in Fig. 6(b), meaning that there exists a strong reaction between ductile Ti particle and shear banding from the amorphous matrix. It directly shows that the bifurcation of shear bands around the Ti particles have been observed in the fractured Mg-based BMGC/40 vol.% Ti particles specimen with 24% plastic strain after compression test, lots of stress concentration was released by the plastic deformation of ductile Ti particles. On the other hand, the fracture surface of the Mg-based BMGC/40 vol.% Ti particles compressive specimen reveals the mixed morphologies, consisting of vein-like pattern and plastically sheared Ti particles, as shown in Fig. 7. In this case, a locally melted region is observed on the fracture surface, indicating that a large amount of strain along the shear band led to localized melting before fracture. In addition, the plastically sheared Ti particles of fracture surface indicate that the energy of shear bands is highly absorbed by these ductile Ti particles. This suggests that the dispersed Ti particles act as a network in the glassy matrix, thus separate and restrict the highly localized shear banding, avoiding catastrophic shearing-off through the whole sample and so as to significantly improve their plasticity.

4. Conclusion

In summary, the Mg-based BMG composites with ductile Ti particles developed in the study may constitute a very promising material for structural applications due to their high compressive plastic strains comparable to that of crystalline alloys and high yield strength comparable to metallic glassy matrix. These dispersed Ti particles can highly absorb the energy of shear banding and branch primary shear band into multiple shear bands, thus decrease the stress concentration for further propagation of shear band and results in drastically enhancing plasticity. Additionally, the Mg-based BMGC with 40 vol.% Ti particles still keeps the high yield strength of 800 MPa because of its good bonding interface between Ti particles and the amorphous matrix. Overall, the ductile Ti dispersoids would provide a good toughening effect in promoting the practical use of amorphous materials.

Acknowledgements

It is grateful to acknowledge the sponsorship by National Science Council of Taiwan, ROC, under the Project Nos. NSC 95-2210-E-214-015-MY3, NSC 96-2218-E-110-001 and NSC 97-2112-M-214-002-MY2. In addition, the authors like to acknowledge the help on SEM and TEM analysis by the Micro and Nano Analysis Laboratory of I-Shou University.

References

[1] A. Inoue, T. Masumoto, Mater. Sci. Eng. A 133 (1991) 6.
[2] H. Ma, J. Xu, E. Ma, Appl. Phys. Lett. 83 (2003) 2793.
[3] X. Hui, W. Dong, G.L. Chen, K.F. Yao, Acta Mater. 55 (2007) 907.
[4] K. Amiya, A. Inoue, Mater. Trans. JIM 41 (2000) 1460.
[5] A. Inoue, N. Nishiyama, H. Kimura, Mater. Trans. JIM 38 (1997) 179.
[6] H. Men, D.H. Kim, J. Mater. Res. 18 (2003) 641.
[7] G. Yuan, A. Inoue, J. Alloys Compd. 387 (2005) 134.
[8] C. Fan, R.T. Ott, T.C. Hufnagel, Appl. Phys. Lett. 81 (2002) 1020.
[9] H.Y. Choi, R. Busch, U. Köster, W.L. Johnson, Acta. Mater. 47 (1999) 2455.
[10] J. Das, M.B. Tang, K.B. Kim, R. Theissmann, F. Baier, W.H. Wang, J. Eckert, Phys. Rev. Lett. 94 (2005) 205501.
[11] D.C. Hofmann, J.Y. Suh, A. Wiest, G. Duan, M.L. Lind, M.D. Demetriou, W.L. Johnson, Nature 451–28 (2008) 1085.
[12] J. Eckert, J. Das, S. Pauly, C. Duhamel, J. Mater. Res. 22 (2007) 285.
[13] A.H. Brother, D.C. Dunand, Q. Zheng, J. Xu, J. Appl. Phys. 102 (2007) 023508.
[14] L. Liu, K.C. Chen, M. Sun, Q. Chen, Mater. Sci. Eng. A445–446 (2007) 697.
[15] Y.K. Xu, H. Ma, J. Xu, E. Ma, Acta Mater. 53 (2005) 1857.
[16] J.S.C. Jang, L.J. Chang, J.H. Young, J.C. Huang, C.Y.A. Tsao, Intermetallics 14 (2006) 945.
[17] P.Y. Lee, C. Lo, J.S.C. Jiang, J.C. Huang, Key Eng. Mater. 313 (2006) 25.
[18] J. Li, L. Wang, H.F. Zhang, Z.Q. Hu, H. Cai, Mater. Lett. 61 (2007) 2217.
[19] D.G. Pan, H.F. Zhang, A.M. Wang, Z.Q. Hu, Appl. Phys. Lett. 89 (2006) 261904.
[20] J.S.C. Jang, J.Y. Ciou, T.H. Hung, J.C. Huang, X.H. Du, Appl. Phys. Lett. 92 (2008) 011930.
[21] M. Kinaka, H. Kato, M. Hasegawa, A. Inoue, Mater. Sci. Eng. A 494 (2008) 29.
[22] J.S.C. Jang, S.R. Jian, T.-H. Li, J.C. Huang, C.Y.A. Tsao, C.-T. Liu, J. Alloys Compd. 485 (2009) 290–294.